Improving fouling resistance of seawater desalination membranes via surface modification

Jong-Min Lee, Hyun-Woong Lee, Yeo-Jin Kim, Hyung-Gyu Park, Sung-Pyo Hong and Ja-Young Koo

ABSTRACT

A commercial polyamide seawater reverse osmosis membrane (Woongjin Chemical CSM) was surface-modified with fluoro-compounds. The effect of this surface modification on both water and NaCl permeability before and after organic fouling was investigated. The structural and electrical characteristics of the membrane surface were measured using atomic force microscopy and electrokinetic analysis respectively. When modified, the membrane surface showed only slight changes to the surface roughness and surface charges. The modified membrane also showed highly improved fouling resistance during cross-flow filtration of characteristic seawater organic foulants (humic acid and sodium alginate). Contact angle analysis using the Owens-Wendt theory was used to calculate the surface energy of the modified membrane. Lower surface energy of the modified membrane was identified as the key factor in the improved fouling resistance of the membranes.

Key words | contact angle, fouling resistance, seawater reverse osmosis membrane, surface energy, surface modification

Jong-Min Lee (corresponding author)
Hyun-Woong Lee
Yeo-Jin Kim
Hyung-Gyu Park
Sung-Pyo Hong
Ja-Young Koo
Woongjin Chemical Co., Ltd,
287, Gongdan-Dong,
Gumi-City,
Kyungbuk,
Korea 730-030
E-mail: *jmlee@wjchemical.co.kr*

INTRODUCTION

With the rise in global population, sea levels, desertification, and industrialization, shortages of freshwater are growing at an alarming rate all around the world. Recently, in order to combat this crisis, there has been a great focus on the development of water reclamation technologies. One of these, seawater desalination, in particular with the use of a reverse osmosis (RO) membrane, has seen a rapid growth in the global market.

In many Middle Eastern countries, Saudi Arabia, the United Arab Emirates, and Kuwait, in particular, desalinated water makes up a major component of their available water resources (Alawadhi 2002; Drinking Water from the Sea 2005). Although thermally driven processes, such as distillation, are used in a majority of their desalination processing plants, most plants built after 1990 utilize the RO membrane separation process due to its lower operational/maintenance costs and smaller environmental footprint. Additionally, this process yields high quality water that is free from harmful factors such as boron (Sarp *et al.* 2008).

Despite the many benefits of using RO for desalination, it is not without problems. During seawater desalination RO processes, the membrane suffers from a build-up of organic matter on its surface, which is referred to as membrane fouling. Fouling by such organic contaminants can cause irreversible damage to the membrane surface that can lower flux performance of the membranes during operation, eventually leading to short membrane lifetimes. Previous studies using RO systems in desalination processes have found that natural organic matter (NOM) is the primary cause of membrane fouling (Ghani *et al.* 2000; Salinas Rodríguez *et al.* 2009). NOM is a heterogeneous mixture of complex compounds including humic substances, hydrophobic acids, carbohydrates, amino acids, carboxylic acids, proteins, and hydrocarbons, all of which are either generated during the biological decomposition of animals and

doi: 10.2166/wrd.2013.000

plants or exist in natural waters (Croué *et al.* 1999). The major characteristic NOM in the RO desalination process includes humic acid and sodium alginate (Jin *et al.* 2009; Salinas Rodríguez *et al.* 2009). They are hydrophilic and hydrophobic, respectively, and can cause variable degrees of fouling based on the characteristics of membrane surface.

Chemical modification of membrane surfaces, via grafting or deposition, for example, has previously been found to impart fouling resistant characteristics to membrane surfaces (Kwak *et al.* 2001; Rana & Matsuura 2010), and there have been many attempts that have focused on increasing the hydrophilicity of the membrane surface for fouling resistance (Hachisuka & Ikeda 2001; Mickols 2001; Koo *et al.* 2009). In addition to improving hydrophilicity, membranes with lower surface roughness have been found to be less prone to fouling (Elimelech *et al.* 1997; Vrijenhoek *et al.* 2001). Membranes with a more neutral surface charge have also been linked to anti-fouling characteristics (Sagle *et al.* 2009). However, many of these methods have been found to impart undesirable characteristics to the membranes, such as reduced flux, lower NaCl rejection, and weaker mechanical properties.

This study focuses on achieving fouling resistance not by increasing hydrophilicity or changing other surface characteristics but by reducing the surface energy of the membrane. Compounds containing fluorine were used to coat polyamide seawater reverse osmosis (SWRO) membranes in order to reduce the surface adhesion of major organic foulants in seawater.

MATERIALS AND METHODS

The anti-foulants used for membrane surface modification in this study were ATFP (1-amino-3-(2,2,3,3-tetrafluoroethoxy)-2-propanol) with four substituted fluorines and AOFP (1-amino-3-(2,2,3,3,4,4,5,5-octafluoropentoxy)-2-propanol) with eight substituted fluorines. These two compounds were synthesized in the laboratory. Their structures are shown in Figure 1.

The surface modification of polyamide SWRO membranes was accomplished through a dip-coating process. Polyamide membranes made by interfacial polymerization were dipped in aqueous anti-foulant solutions of various

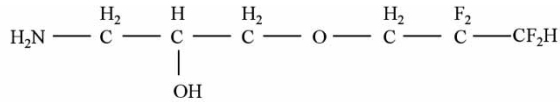

1-Amino-3-(2,2,3,3-tetrafluoropropoxy)-2-propanol

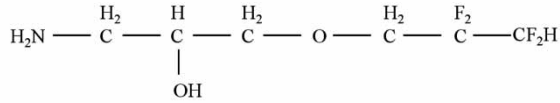

1-Amino-3-(2,2,3,3,4,4,5,5-octafluoropentoxy)-2-propanol

Figure 1 | Structures of the fluoro-compounds used for surface modification.

ATFP and/or AOFP concentrations and other additives for 40 s. Then the membranes were stored in a 0.2wt% sodium carbonate aqueous solution for 2 h then soaked in deionized water for 30 min prior to testing.

The hydrophilicity of the membrane surface was measured by the sessile drop method using a contact angle analyzer (VCA Optima, AST Products Inc.). The reported contact angle values are average values from four separate sessile drop images for each membrane sample. An electrokinetic analysis (EKA) (electrokinetic analyzer; Brookhaven Instruments Corp.) was used to measure the surface charge of the modified membranes. The electrical potential of the surface was measured in the range pH 4–11 in a 5 mM NaCl solution. The reported EKA curve is an average of two separate measurements. The surface roughness of the membranes was analyzed by atomic force microscopy (AFM; Autoprobe M5, Park Scientific Instruments). The reported surface roughness values are average values from three separate images for each membrane sample. Surface energy of each membrane sample was analyzed using a tensiometer (Processor-Tensiometer K100, KRUSS) with deionized water, diiodomethane, and ethylene glycol as the probe liquids. The Owens-Wendt theory was used to calculate the surface energy values and is shown in the following equation:

$$\frac{\sigma_L(\cos\theta+1)}{2\sqrt{\sigma_L^D}}=\frac{\sqrt{\sigma_S^P}\sqrt{\sigma_L^P}}{\sqrt{\sigma_L^D}}+\sqrt{\sigma_S^D} \quad (1)$$

where θ is the measured contact angle, σ_L is the total surface energy of the liquid, σ_L^D and σ_L^P are the dispersive and polar

components of the liquid surface energy, σ_S^D and σ_S^P are the dispersive and polar components of the surface (Owens & Wendt 1969).

Flux and rejection values of each flat sheet membrane sample were evaluated using a constant transmembrane pressure cross-flow filtration system (effective filtration area ≈3.5 inch^2; 1 inch = 2.54 cm). The cross-flow system was operated at 800 psi with a cross-flow rate of 1 gal/min (1 gallon = 3.785 litres). The feed temperature was maintained at 25 °C and the pH was maintained at 8. The feed solution was a simulated seawater mixture with NaCl concentration of 32,000 ppm. Permeate samples were collected for 30 min after 1 h of steady-state operation. The samples were then weighed and measured for conductivity. The flux was calculated from the following equation:

$$J_w = \frac{\Delta M}{\Delta t}\frac{1}{\rho_w A} \quad (2)$$

where J_w is the permeate water flux, ΔM is the permeate mass change over filtration time of Δt, ρ_w is the density of water, and A is the effective filtration area of the membrane sample. NaCl rejection was calculated from the following equation:

$$R = \left(1 - \frac{C_p}{C_F}\right) \times 100 \quad (3)$$

where R is the NaCl rejection, C_p is the conductivity of the permeate, and C_F is the conductivity of the feed.

Fouling resistance of the membrane sample was evaluated by adding 2 ppm of calcium chloride, 10 ppm of sodium alginate (Wako) and/or 10 ppm of humic acid (Aldrich) to the feed solution and measuring the flux decline over a period of 2 h. Flux decline was calculated using the following equation:

$$\text{Flux decline}(\%) = \left(\frac{J}{J_0} - 1\right) \times 100 \quad (4)$$

where J_0 is initial flux before fouling and J is the flux of the membrane after fouling.

A constant transmembrane pressure testing skid was used to test 8-inch module elements. The system was operated at 800 psi with a recovery rate of 8%. The feed temperature was maintained at 25 °C and the pH was maintained at 8. The feed solution was a simulated seawater mixture with NaCl concentration of 32,000 ppm and boron concentration of 5 ppm. The flux was measured by a built-in flow meter and NaCl rejection was calculated using Equation (3) as previously described. Boron rejection was measured using an auto-analyzer (swAAt, BLTEC Co., Tokyo).

RESULTS AND DISCUSSION

In order to first select the appropriate anti-foulant compound for use in a full-scale 8-inch element, an initial laboratory study was conducted using both ATFP and AOFP as surface modifiers. Table 1 shows the permeate flux and contact angles of these ATFP- and AOFP-modified membranes. All of the modified RO membranes had significant permeate flux reduction in comparison with the control membrane. The flux decrease was larger for AOFP modifications that had eight fluorine substituents than for ATFP modifications with only four fluorine substituents. Additionally, as concentrations of the fluorinated compounds used in the modifications increased, the membranes had larger losses in flux performance. This is probably due to the increasing hydrophobic interactions by the added fluorine grafts which can interrupt the passage of water at the membrane surface. These findings were consistent with the contact angle analysis. When more fluorine groups attached to the membrane surface, hydrophobicity rose significantly. Contact angle measurements were higher with AOFP than

Table 1 | Comparison of permeate flux and contact angle of ATFP- and AOFP-modified membranes

No.	Surface modification	Flux (GFD)[a]	NaCl rejection (%)	Contact angle (°)
1	Control	26.03	99.51	46.8
2	0.01% ATFP	17.53	99.58	118
3	0.05% ATFP	15.07	99.59	–
4	0.1% ATFP	13.63	99.63	126.3
5	0.01% AOFP	15.92	99.60	126.8
6	0.05% AOFP	9.17	99.57	–
7	0.1% AOFP	8.45	99.63	140.6

[a]Gallons per square foot per day (1 GFD = 1.7 litres per square metre per day).

with ATFP and with increasing concentration of the fluorocompounds used in the modification.

Figure 2 shows the flux decline of the modified membranes after 2 h of fouling. As expected, the surface modified membranes all had better fouling resistance than the control membrane. Additionally, this was extremely evident in the sodium alginate fouling, where the surface coatings on average showed three times less flux decline than the control membrane. Because both ATFP and AOFP showed similar resistance to fouling by humic acid and sodium alginate, ATFP which had a smaller impact on the permeate flux was chosen as the primary anti-foulant compound for the SWRO surface modification.

Prior to utilizing the ATFP anti-foulant for a full-scale 8-inch element, it was determined that the ATFP treatment on its own had too much impact on the permeate flux of the RO membrane. Therefore, a flux-enhancing additive was added to the surface modification. The dip-coating process remained the same but a small amount of additive was added to the aqueous ATFP solution.

Figure 3 shows the flux decline of this ATFP + additive modified membrane charted as a function of time during cross-flow filtration of a characteristic seawater foulant solution (32,000 ppm NaCl, 5 ppm boron, 10 ppm humic acid, 10 ppm sodium alginate, and 2 ppm $CaCl_2$). A clean in place (CIP) cycle was conducted at hours 3, 5, and 7 using a 0.2% NaOH solution at 225 psi. As expected, the surface-modified membrane showed flux declines that were about half of that of the control membrane. But the most impactful advantage was the recovery of the membrane flux after CIP cycles. As seen at hours 3, 5, and 7, the modified membrane was able to recover its flux back to or sometimes to levels even higher than the starting flux prior to fouling. In comparison, the control membrane slowly loses its ability to recover its flux after CIP cycles and suffers a more dramatic flux decline over the same foulant filtration cycle. NaCl rejection properties of both the control and modified membranes remained above 99.5% and did not change during the entirety of the cross-flow filtration.

Table 2 shows the results of surface roughness analysis on ATFP + additive modified membranes. R_{p-v} shows the difference between the highest and lowest points within the illuminated area. R_{ave} is the mean-variance of discrepancies between roughness at each pixel based on average height Z_0 in the illuminated area as shown in Equation (5). Here, S is illuminated area and $f(x,y)$ is the coordinate of height at each area; a and b represent horizontal and vertical lengths; Z_0 is the average height, which is shown in Equation (6); R_{rms} is the squared mean-variance of discrepancies between roughnesses at each pixel based on Z_0 in the illuminated area shown by Equation (7):

$$R_{ave} = \frac{1}{S}\int_0^a\int_0^b |f(x,y) - Z_0|\, d_x d_y \tag{5}$$

$$Z_0 = \frac{1}{S}\int_0^a\int_0^b f(x,y) d_x d_y \tag{6}$$

$$R_{rms} = \left[\frac{1}{S}\int_0^a\int_0^b |f(x,y) - Z_0|^2 d_x d_y\right]^2 \tag{7}$$

In terms of the relationship between a membrane's fouling resistant characteristics and surface roughness, smooth membranes are reported to be less susceptible to fouling than rough membranes (Elimelech *et al.* 1997). The ATFP + additive modification had a slightly less rough surface than

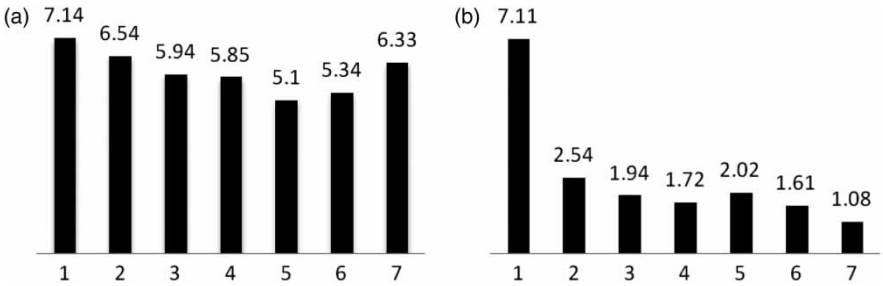

Figure 2 | Flux decline of modified membranes after 2 h of fouling represented as percentages. (a) Flux decline during humic acid fouling (10 ppm humic acid + 2 ppm $CaCl_2$); (b) flux decline during sodium alginate fouling (10 ppm sodium alginate + 2 ppm $CaCl_2$).

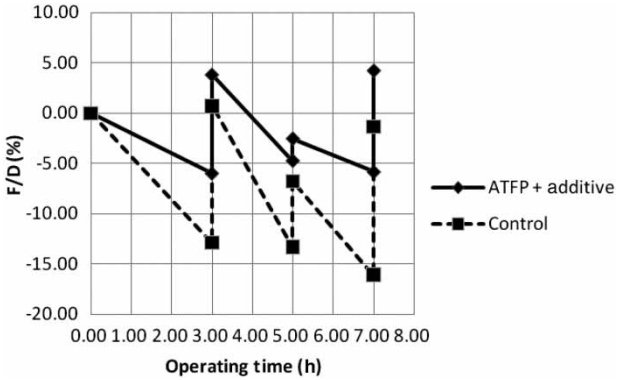

Figure 3 | Flux decline as a function of time during cross-flow filtration of foulants (10 ppm sodium alginate, 10 ppm humic acid, and 2 ppm $CaCl_2$). A CIP cycle using a 0.2% NaOH solution was conducted at 3, 5, and 7 h.

Table 2 | Atomic force microscopy analysis of surface modification

Surface modification	$R_{p\text{-}v}$(nm)	R_{rms}(nm)	R_{ave}(nm)	Surface area (nm^2)
Control	578.20	64.60	51.73	757.10
ATFP + additive	555.73	58.42	46.44	758.33

the control membrane, but the difference was not significant. Although the anti-fouling effect may be assisted by this less rough surface, it would be an exaggeration to say that the majority of the anti-fouling properties of the surface modification could be attributed to this change in surface morphology.

Streaming potential analysis is often used to analyze the electrical characteristics of RO membranes. Streaming potential difference can intensify concentration polarization at the surface of membrane to cause the foulants to deposit on the membrane. Generally, forms of organic matter with positive charges are more likely to be attracted to carboxylic acid groups with negative charge on the surface of membrane. Therefore, a more neutral surface is generally a favorable characteristic of anti-fouling membranes. Figure 4 shows the EKA analysis of the ATFP + additive modified membranes in comparison to the control RO membrane. In terms of surface charge, there does not seem to be a significant change between the modified and control membranes. Rather, the control membrane has a more neutral surface than the modified membrane which indicates that the ATFP treatment does not impart its anti-fouling properties due to surface charge differences.

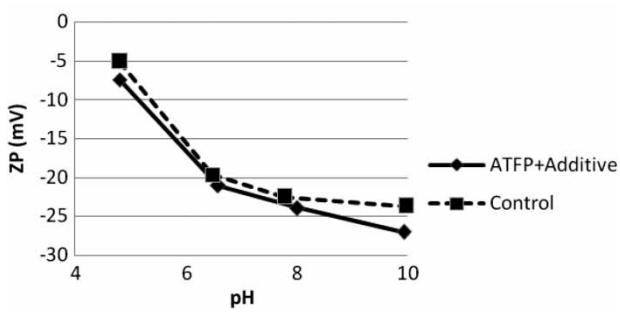

Figure 4 | EKA analysis of surface modified membrane.

The interaction between the membrane surface and the foulants in solution is the key determinant of fouling. Lower surface free energy during the adsorption of foulants onto the membrane surface results in fouling resistance of the membranes (Choo & Lee 2000). A tensiometer using three different probe liquids (deionized water, diiodomethane, and ethylene glycol) was used to take surface energy measurements. As calculated by the Owens-Wendt theory, the surface energy was 67.29 mJ/m^2 for the ATFP + additive modified membrane and 48.62 mJ/m^2 for the control membrane; thus surface energy was reduced by about 30% in the modified membrane. Because this surface modification does not impart major changes to the roughness or charge characteristics of the membrane, the key anti-fouling mechanism for the ATFP coating is its ability to reduce the available surface free energy. This change allows for the membrane to resist major organic fouling by reducing overall adhesion of foulants on the surface. This result echoes back to the flux recovery seen after the CIP process, which is an indication of the weaker adhesion forces between the foulants and the membrane surface.

With the ATFP + additive surface modification properly characterized in laboratory-scale testing, a full-scale 8-inch module element was rolled and tested in a cross-flow testing skid. Table 3 is a summary of its performance in comparison

Table 3 | Surface modified 8-inch module element performance

Surface modification	Flux (GPD)[b]	Rej. (%)	Boron rejection (%)	Flux decline (%)
Control	7,368	99.75	92.5	5.54
ATFP + additive	7,457	99.75	92.1	2.5
Control[a]	7,500	99.75	92	–

[a]Catalog specifications.
[b]GPD = Gallons per day (1 GDP = 3.785 litres per day).

with that of a standard SWRO element. Overall, the ATFP + additive surface modification yielded an SWRO membrane element comparable to an existing commercial element. Permeate flux, NaCl rejection, and boron rejection of the surface-modified element were all within the necessary specifications while showing a flux decline during fouling half of that of the control membrane. Further field testing of the ATFP-surface-modified elements is to be conducted in the near future.

CONCLUSIONS

A commercial polyamide SWRO membrane (Woongjin Chemical CSM) was surface-modified with fluoro-compounds. The effect of this surface modification on both water and salt permeability before and after organic fouling was investigated. The water permeability of the surface modification significantly reduced the flux of the SWRO membrane during cross-flow filtration, while having negligible effects on NaCl permeability. The structural and electrical characteristics of the membrane surface were measured using AFM and EKA respectively. When modified, the membrane surface showed a slightly decreased surface roughness and was slightly more negative. The modified membrane also showed improved fouling resistance during cross-flow filtration of characteristic seawater organic foulants (humic acid and sodium alginate). By altering the surface modification formula with addition of a flux-enhancing additive, the flux performance of the SWRO membrane was maintained while the anti-fouling properties of the ATFP compound still continued to be effective. Surface energy analysis of the modified and unmodified membrane samples showed that the key determining anti-fouling effect of the ATFP compound was the 30% reduction in available surface free energy. This lowered the adhesion of major organic foulants which was especially evident after the flux recovery after CIP cycles during foulant filtration. Testing of the 8-inch-module element provided further evidence that this surface modification met both the flux and rejection standards in the field while enhancing the element's anti-fouling properties.

ACKNOWLEDGEMENT

This research was supported by a grant (code #07SeaheroB02-02) from the Plant Technology Advancement Program funded by the Ministry of Land, Transport and Maritime Affairs of the Korean government.

REFERENCES

Alawadhi, A. A. 2002 Regional Report on Desalination-GCC Countries, *Proceedings of the IDA World Congress on Desalination and Water Reuse*, Manama, Bahrain, pp. 8–13.

Choo, K. H. & Lee, C. H. 2000 Understanding membrane fouling in terms of surface free energy changes. *J. Colloid Interface Sci.* **226**, 367–370.

Croué, J.-P., Violleau, D., Bodaire, C. & Legube, B. 1999 Removal of hydrophobic and hydrophilic constituentsby anion exchange resins. *Water Sci. Technol.* **40**, 207–214.

Drinking Water from the Sea 2005 Middle East Electricity, April 2005, pp. 21–22.

Elimelech, M., Zhu, X., Childress, A. E. & Hong, S. 1997 Role of membrane surface morphology in colloidal fouling of cellulose acetate and composite aromatic polyamide reverse osmosis membranes. *J. Membr. Sci.* **127**, 101–109.

Ghani, A., Dalvi, I., Al-Rasheed, R. & Javeed, M. A. 2000 Studies on organic foulants in the seawater feed of reverse osmosis plants of SWCC. *Desalination* **132**, 217–232.

Hachisuka, H. & Ikeda, K. 2001 Composite reverse osmosis membrane having a separation layer with polyvinyl alcohol coating and method of reverse osmotic treatment of water using the same, US Patent, 6177011.

Jin, X., Huang, X. & Hoek, E. M. 2009 Role of specific ion interaction in seawater RO membrane fouling by alginic acid. *Environ. Sci. Technol.* **43**, 3580–3587.

Koo, J.-Y., Hong, S. P., Lee, J. H. & Ryu, K. Y. 2009 Selective membrane having high fouling resistance, US Patent, 7537697.

Kwak, S. Y., Kim, S. H. & Kim, S. S. 2001 Hybrid organic/inorganic reverse osmosis (RO) membrane for bactericidal anti-fouling. 1. Preparation and characterization of TiO2 nanoparticle self-assembled aromatic polyamide thin-film-composite (TFC) membrane. *Environ. Sci. Technol.* **35**, 2388–2394.

Mickols, W. E. 2001 Composite membrane with polyalkylene oxide modified polyamide surface, US Patent, 6280853.

Owens, D. K. & Wendt, R. C. 1969 Estimation of the surface free energy of polymers. *J. Appl. Polym. Sci.* **13**, 1741.

Rana, D. & Matsuura, T. 2010 Surface modification for antifouling membrane. *Chem. Rev.* **110**, 2448–2471.

Sagle, A. C., Van Wagner, E. M., Ju, H., McCloskey, B. D., Freeman, B. D. & Sharma, M. M. 2009 PEG-coated reverse osmosis membranes: desalination properties and fouling resistance. *J. Membr. Sci.* **340**, 92–108.

Salinas Rodríguez, S. G., Kennedy, M. D., Schippers, J. C. & Amy, G. L. 2009 Organic foulants in estuarine and bay sources for seawater reverseosmosis – comparing pre-treatment processes with respect to foulant reduction. *Desalination Water Treat.* **9**, 155–164.

Sarp, S., Lee, S., Ren, X., Lee, E., Chon, K., Choi, S. H., Kim, S., Kim, I. S. & Cho, J. 2008 Boron removal from seawater using NF and RO membranes, and effects of boron on HEK 293 humanembryonic kidney cell with respect to toxicities. *Desalination* **223**, 23–33.

Vrijenhoek, E. M., Hong, S. & Elimelech, M. 2001 Influence of membrane surface properties on initial rate of colloidal fouling of reverse osmosis and nanofiltration membranes. *J. Membr. Sci.* **188**, 115–128.

First received 21 November 2012; accepted in revised form 28 January 2013. Available online 21 March 2013